Structure 14, 309–319, February 2006 ©2006 Elsevier Ltd All rights reserved DOI 10.1016/j.str.2005.11.012

Molecular Basis for Phosphorylation-Dependent, PEST-Mediated Protein Turnover

Maria M. García-Alai,[1,4] Mariana Gallo,[2,4] Marcelo Salame,[1] Diana E. Wetzler,[1] Alison A. McBride,[3] Maurizio Paci,[2] Daniel O. Cicero,[2] and Gonzalo de Prat-Gay[1,*]
[1]Instituto Leloir
Patricias Argentinas 435
(1405) Buenos Aires
Argentina
[2]University of Rome 'Tor Vergata'
via della Ricerca Scientifica
00133, Rome
Italy
[3]Laboratory of Viral Diseases
National Institute of Allergy and Infectious Disease
National Institutes of Health
Bethesda, Maryland 20892-0455

Summary

Proteasomal-mediated rapid turnover of proteins is often modulated by phosphorylation of PEST sequences. The E2 protein from papillomavirus participates in gene transcription, DNA replication, and episomal genome maintenance. Phosphorylation of a PEST sequence located in a flexible region accelerates its degradation. NMR analysis of a 29 amino acid peptide fragment derived from this region shows pH-dependent polyproline II and α helix structures, connected by a turn. Phosphorylation, in particular that at serine 301, disrupts the overall structure, and point mutations have either stabilizing or destabilizing effects. There is an excellent correlation between the thermodynamic stability of different peptides and the half-life of E2 proteins containing the same mutations in vivo. The structure around the PEST region appears to have evolved a marginal stability that is finely tunable by phosphorylation. Thus, conformational stability, rather than recognition of a phosphate modification, modulates the degradation of this PEST sequence by the proteasome machinery.

Introduction

The biological activities of key proteins are often regulated by intracellular levels, which result from a balance between synthesis and degradation. Rapid turnover is a regulatory mechanism that has evolved for many proteins, such as metabolic enzymes, transcription factors, and cell cycle regulators (Rechsteiner, 1991), which are involved in processes ranging from primitive mechanisms of development (Belvin et al., 1995) to disease (Martinez et al., 2003). In 1986, Reichsteiner and Rogers described the existence of small peptide motifs that target proteins for degradation. Such regions are rich in proline (P), glutamate (E) or aspartic acid, serine (S), and threonine (T) and were defined as PEST motifs (Rogers et al., 1986). Since then, different sequences that do not contain the PEST motif have also been shown to function as proteolytic signals. These motifs, rich in prolines, poly-alanine, poly-glutamic acid, and poly-lysine residues, are required for targeting a vast number of proteins for degradation (Reichsteiner and Rogers, 1996), but less is known about the mechanism for protein recognition by the proteolytic machinery. Many PEST-containing proteins are known to be degraded by the ubiquitin-26S proteasome (Rechsteiner, 1991), and therefore they must be recognized by the U2/U3 ligase system to become substrates for proteolysis. However, although the PEST motif is present all the time, the protein is not recognized until it is "marked" for degradation. Different molecular mechanisms such as ligand binding (Shumway et al., 1999), exposure to light, and phosphorylation (Rechsteiner, 1990) have been described for activating this process. How these degradation signals are presented to the proteolytic machinery is not known, nor is the role of this sequence in protein stability and protein-protein recognition.

Papillomaviruses are small DNA viruses that infect epithelia and cause lesions known as papillomas or warts, and a subset of human viral types are linked to the development of cervical cancer. Bovine papillomavirus type 1 has been studied as a prototype for genetic analysis of all papillomaviruses (Howley, 2001). The viral E2 protein is crucial for the viral life cycle since it regulates viral gene transcription and is required for viral DNA replication, genome maintenance, and chromosomal segregation (Skiadopoulos and McBride, 1998). The 410 residue full-length E2 protein consists of two conserved functional domains, an N-terminal transactivation domain and a C-terminal DNA binding and dimerization domain, that are separated by a nonconserved region of ~80–100 residues defined as "the hinge region." The hinge region is considered to be flexible and unstructured (Gauthier et al., 1991), and it includes a PEST motif (residues 290–310) that contains phosphorylation sites S298 and S301 (Figure 1) (McBride and Howley, 1991). Nevertheless, no structural data are available for this region either in isolation or in constructs containing either or both N- and C-terminal domains.

Phosphorylation of S301 targets E2 for degradation, and its replacement with alanine results in a protein with increased half-life and reduced levels of ubiquitination (Penrose and McBride, 2000). An extensive mutational analysis of the PEST region showed that substitution of glutamic acid residues 303 and 304 triggered E2 for degradation independent of phosphorylation of residue 301. In addition, substitution of residue P299 with alanine largely increased the in vivo half-life of the protein even when S301 was phosphorylated (Penrose et al., 2004). Therefore, it was concluded that it is not the phosphate moiety that is recognized by the proteasome system, but rather a conformational switch that affects the local thermodynamic stability of the protein, resulting in its degradation. Structural studies confirmed that phosphorylation induced conformational changes in

*Correspondence: gpratgay@leloir.org.ar
[4]These authors contributed equally to this work.

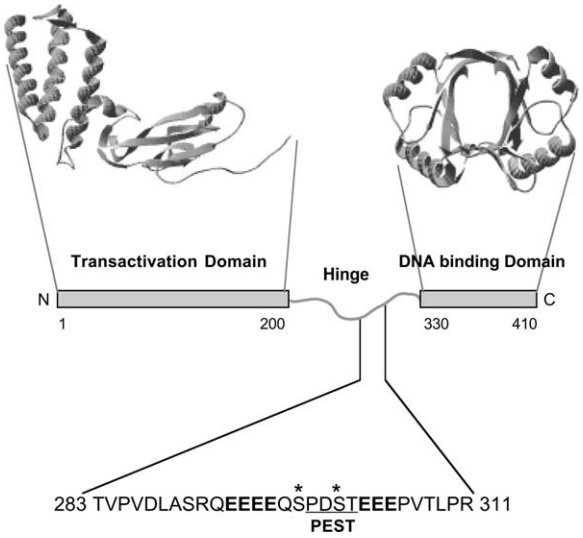

Figure 1. Domain Arrangement of the BPV1 E2 Protein and Localization of the PEST Motif

Full-length E2 consists of two structural domains, the transactivation domain (left) and the DNA binding and dimerization domain (right) connected by a nonconserved region defined as the "hinge," corresponding to residues 200–330. The peptide E2-PEST (283–311) contains the PEST switch region (underlined), poly-glutamic regions (bold), and serines 298 and 301 (*) that can be phosphorylated by CKI and CKII.

peptides corresponding to the hinge region (Penrose et al., 2004).

In this work, we show that the unphosphorylated synthetic peptide spanning the PEST region in this "flexible connector" contains regions of polyproline-type (PII) and residual α helix structures that are perturbed by phosphorylation. PII has been proposed to be the main conformation of unstructured proteins (Shi et al., 2002b), but the assignment of PII in polypeptides is not as direct as for the canonical secondary structures such as α helices, β sheets, or turns. Here, we present NMR and circular dichroism data showing that phosphorylation of residue 301 modifies the local stability of the E2-PEST peptides, thus disturbing both the PII conformation and the overall structure and leading to increased degradation of the E2 protein within the cell.

Results

The E2-PEST Peptide Is a Natural Poly-Glutamic Model

The BPV1 E2 "hinge" domain (residues 200–310) includes a region rich in glutamic acid residues containing the PEST degradation sequence (Penrose and McBride, 2000). Figure 1 shows the sequence of the synthetic peptide used in our studies and its location in the context of the full-length protein. Phosphorylation sites (S298 and S301), located in the PEST region between two poly-E tracts, are also highlighted. Poly-glutamic model peptides are known to adopt a polyproline II (PII)-like, left-handed helical conformation, and this type of structure undergoes a pH transition that can be followed by circular dichroism (Tiffany and Krimm, 1968). Therefore, we investigated the possible presence of PII in this peptide.

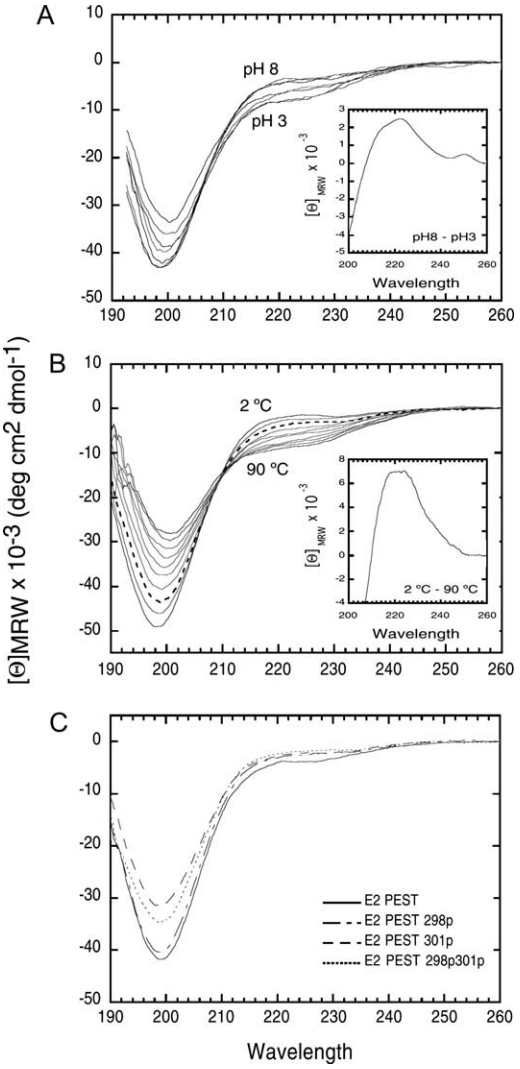

Figure 2. Far-UV Circular Dichroism of the E2-PEST Peptide and the Phosphorylated Forms

(A) E2-PEST at different pHs. Inset: differential spectrum of E2-PEST between pH 8.0 and pH 3.0.

(B) E2-PEST at pH 7.5 at different temperatures; the spectrum at 20°C is shown as a dotted line. Inset: differential spectrum of E2-PEST between 2°C and 90°C.

(C) E2-PEST (full line), E2-PEST298p (broken line), E2-PEST301p (dashed line), and E2-PEST298p301p (dotted line) in 10 mM Tris-HCl (pH 7.5).

A far-UV CD spectrum for peptides with PII displays a minimum at 198 nm, a negative band at 228 nm, and a positive distinctive band at around 218 nm at neutral pH (Shi et al., 2002a). The CD spectrum of the E2-PEST peptide presents such characteristics at pH 8.0, which disappear as a result of the neutralization of the acidic side chains upon a decrease in pH (Figure 2A, also see inset). In addition, PII-type helices are sensitive to temperature, providing further evidence for their presence (Tiffany and Krimm, 1972). The E2-PEST peptide displays maximum PII-type behavior at 2°C and minimum PII-type behavior at 90°C; the difference spectra further

uncover the spectral features, with the characteristic broad band around 218 nm (Figure 2B, also see inset).

When assessed separately, the phosphorylated forms of E2-PEST at S298 (E2-PEST298p) and S301 (E2-PEST301p) appeared fully disordered; however, their spectra show considerable differences in molar ellipticity compared to the unphosphorylated peptide (Figure 2C). E2-PEST301p appears to have its PII content disrupted, while E2-PEST298p displays a negative molar ellipticity value at 198 nm almost indistinguishable from the unphosphorylated peptide. When molar ellipticity at 220 nm of the three peptides as a function of temperature was followed, all three showed linear decreases, indicating the absence of persistent tertiary cooperative interactions (data not shown).

Stabilization of the PII Conformation in the Unphosphorylated E2-PEST Peptide

Regions of PII in polyglutamic models can be stabilized by addition of the denaturant guanidine chloride (Gdm.Cl), which shifts the equilibrium to the PII population (Tiffany and Krimm, 1973). E2-PEST shows such a behavior when titrated with increasing denaturant concentrations; the positive band at around 218 nm increases with Gdm.Cl concentration (Figure 3A). In contrast, only a small change is observed for E2-PEST301p (Figure 3B), thus strongly suggesting that the presence of the phosphate modification in S301 disrupts the PII structure. The coil-PII transition can be approached as a two-state transition, and the stability of the PII structure, ΔG of PII formation in water, is estimated from a Gdm.Cl titration (Figure 3C, see Experimental Procedures). The unavoidable low signal-to-noise ratio due to the small change and the presence of denaturant introduces a large error, but we can estimate a ΔG of +1.0 kcal mol^{-1} for E2-PEST, whereas the structure stabilization for E2-PEST301p is negligible (Figure 3C; Table 1). An extinction coefficient for PII structures in longer peptides has not yet been obtained, and other contributions to the spectra are expected (Liu et al., 2004).

However, an estimate of the PII population can be obtained from the ΔG values from the two-state model for Gdm.Cl titration assumed (Figure 3; Table 1). The E2-PEST reference peptide shows 16% of its residues in PII conformation, corresponding to 4.8 residues. E2-PEST298p shows 12%, i.e., 3.6 residues, and E2-PESTP299A shows 10%, i.e., 3 residues in PII. Both E2-PEST301p and the doubly phosphorylated peptide are so disrupted that no structure can be stabilized with Gdm.Cl (Figures 3B and 3C). Finally, E2-PESTE304Q approaches 0 residues in the PII conformation. Due to the limitations of the technique, including the lack of models and an inherent low signal-to-noise ratio, these values carry errors up to 50%. Despite that, there appear to be ~4 residues in the PII conformation that are completely disrupted by phosphorylation of S301.

As described before, the rate of degradation of BPV1 E2 in vivo was largely increased by phosphorylation at S301 (Penrose et al., 2004). However, substitution of proline 299 with alanine increases the half-life of E2 by ~30 min (Table 1), but it does not affect phosphorylation. On the contrary, the E304Q mutation results in an extremely unstable protein ($t_{1/2}$ of 24 min, Table 1), but it does not require phosphorylation for rapid degradation (Penrose et al., 2004). Since the half-lives of full-length proteins in vivo are calculated by using Western blot, the half-lives of single and double-phosphorylated forms cannot be determined because of the lack of an antibody that distinguishes them from the unphosphorylated species. The same quantitative analysis of in vivo half-lives shows that replacement of S301 by Ala, increases the half-life to 98 min.

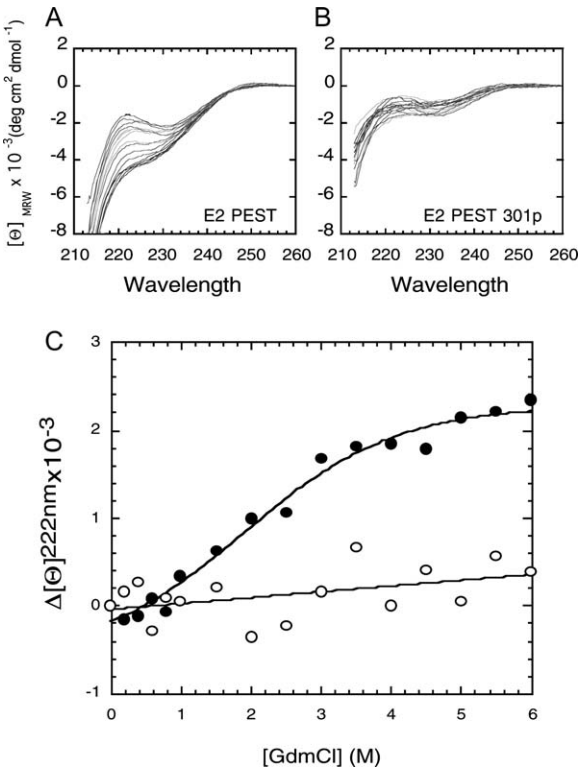

Figure 3. Presence of Regions Containing PII in E2-PEST Peptides; Effect of Phosphorylation

(A and B) Far-UV CD spectra of (A) E2-PEST and (B) E2-PEST301p in the presence of different concentrations of Gdm.HCl at pH 7.5. A positive band around 218 nm is stabilized as the concentration of the denaturant is increased for E2-PEST.

(C) Difference molar ellipticity at 222 nm of E2-PEST (black circle) and E2-PEST301p (white circle) as a function of [Gdm.Cl]. E2-PEST presents a cooperative transition, while no effect is observed for E2-PEST301p. The ellipticity change for PII was followed at 222 nm because of the inherent noise introduced by the high concentrations of denaturant around 215 nm.

In order to analyze the correlation between half-lives and thermodynamic stability, peptides containing these two mutations, E2-PESTP299A and E2-PESTE304Q, were synthesized and analyzed for their PII content (Table 1). The P299A peptide shows no modification of PII content, but it is completely disrupted in the E304Q peptide, probably to a similar extent to that resulting from S301 phosphorylation, which was not determinable (Figure 3C; Table 1).

Regions of Preexisting α Helices in E2-PEST Peptides

The fact that 2,2,2 trifluoroethanol (TFE) is able to stabilize preexisting α-helical populations in peptides has

Table 1. Parameters for PII and α Helix Stabilization in E2-PEST Peptide Variants

Peptide	E2 $t_{1/2}$[a] (min)	ΔG[b] PII, pH 7.5	ΔG α Helix, pH 4.5	% Helix, H_2O	Nα[c], H_2O	% Helix, TFE	Nα, TFE	m, TFE[d]
E2-PEST	63	1.0 ± 0.4	0.96 ± 0.07	15.3 ± 1.8	4.4	38.1 ± 0.3	11	0.34 ± 0.02
E2-PEST298p	Nd[e]	1.2 ± 0.1	1.08 ± 0.07	12.8 ± 1.3	3.7	34.7 ± 0.2	10	0.37 ± 0.02
E2-PEST301p	Nd[e]	Nd	1.09 ± 0.04	12.6 ± 0.9	3.6	29.6 ± 0.1	8.5	0.37 ± 0.01
E2-PEST298p301	Nd[e]	Nd	1.03 ± 0.11	13.9 ± 2.3	4	23.7 ± 0.2	7	0.36 ± 0.02
E2-PESTP299A	94	1.3 ± 0.4	0.88 ± 0.06	17.4 ± 1.5	5	66.3 ± 0.7	19	0.36 ± 0.01
E2-PESTE304Q	24	4.3 ± 2.0	0.99 ± 0.09	14.6 ± 2.1	4.2	42.9 ± 0.3	13	0.39 ± 0.02

Nd, not determinable.
[a] Protein half-lives for full-length E2 wild-type and P299A and E304Q mutants; data presented in Penrose et al. (2004) and quantified with a Kodak ImageStation 440CF and Kodak Digital Science 1D software were used.
[b] ΔG is given in kcal(mol)$^{-1}$.
[c] Nα, number of residues in the α helix.
[d] kcal mol^{-1} M^{-1}.
[e] See main text.

been extensively described (Nelson and Kallenbach, 1986; Buck, 1998). A TFE binding model in which a two-state transition governs the stabilization of helical regions allows the calculation of the parameters of the transition: ΔG; the percent of α helix in water and in TFE; and the m value that describes the effectiveness of the solvent in the interconversion between the two states (Sancho et al., 1992) related in chemical denaturation terms to the differential exposure to the solvent (Myers et al., 1995). To investigate how phosphorylation affects the formation of α-helical structure in the E2-PEST reference peptide, we carried out TFE titrations as shown in Figure 4. The development of the characteristic negative bands around 208 and 222 nm indicate that regions of α helix structure are stabilized in all peptides. We show the unphosphorylated and S301-phosphorylated peptides as the most indicative examples (Figures 4A and 4B). The isodichroic point present in all transitions supports the two-state equilibrium approximation.

The stability of α helix structures present in all E2-PEST peptides is similar (~1 kcal mol^{-1}), which, together with the coincident m values, is a strong indication that the α-helical regions involved are equivalent (Table 1). The residues involved in the PII structure appear either not to be involved or do not produce significant restrictions on the nucleation of the α helix, with the exception of the P299A peptide described below. The amount of α-helical population extrapolated to water ranges from 12.6% to 17.4% depending on the peptide (Table 1). Overall, the changes are small for singly and doubly phosphorylated peptides, and for the E304Q mutation, but they indicate lower helical content (Table 1). The P299A mutation shows a 14% increase in α helix in water, presumably due to the removal of the α helix breaking P299. The α helix in water corresponds to a dynamic interconverting helix, although fewer residues are likely to be involved in the residual α helix present; thus, the values reported (3.6%–5.0%) are likely to be averages to some extent.

Unlike the dynamic α helix present in water, the helix stabilized with 50% TFE represents a consolidated structure and the percent helix calculated provides the number of residues involved in α helix (Chen et al., 1974) (Table 1). At 50% TFE, the unphosphorylated E2-PEST peptide shows 38% α helix, which corresponds to 11 residues. Phosphorylation of S301 causes a decrease in the maximum α helix content to 29.6%, corresponding to 8.5 residues, and phosphorylation of S298 leaves 10 residues. The doubly phosphorylated form of the peptide displays 7 residues in α helix, suggesting a negative-cooperative effect of the two phosphorylation sites under conditions of a consolidated α helix in TFE.

The E304Q mutation shows almost an identical number of residues in α helix (Table 1), but the P299A mutation, showed to dramatically extend the in vivo half-life, increased its thermodynamic stability to 66% of the residues (19 residues) involved in α helix. This corresponds to a 74% increase in α helix content in TFE as opposed to only a 14% increase in water. This is a strong indication that when the helix-breaking proline is replaced by the helix-stabilizing alanine, the helix is extended beyond its natural range.

Structural Details of the E2-PEST Peptide in Solution

CD spectroscopy indicated the presence of both the PII and α helix conformations for the PEST peptide. We decided to use NMR spectroscopy for defining these secondary structure elements within the PEST peptide. For this, we used a combination of NOE experiments, consisting of chemical shift analysis and measurement of scalar coupling constants ($^1J_{CH\alpha}$ and $^3J_{NHH\alpha}$). In addition, we studied the peptide conformation in different environments, such as TFE, water, and Gdm.Cl solutions, and at 10ºC and 25ºC.

Chemical shift analysis of the H_α, C_α, and C_β resonances of the E2-PEST peptide was carried out at 25ºC in the presence of 50% TFE (pH 4.5). Negative variations with respect to reference random coil values for H_α and C_α, and positive values for C_β, are indicative of α helix (Wishart and Sykes, 1994). Based on the observed chemical shift differences, the peptide adopts an α-helical conformation for the 11 residues between V286 and E296 (Figures 5B–5D), in excellent agreement with the CD-TFE titration data (Table 1). The presence of an α helix in V286-E296 is further supported by the $^3J_{NHH\alpha}$ and the $^1J_{CH\alpha}$ coupling constants (Table 2). α-Helical residues have, on average, relatively large $^1J_{CH\alpha}$ values (146.5 ± 1.8 Hz) (Vuister et al., 1992) and small $^3J_{NHH\alpha}$ values (4.0 ± 1.0 Hz) (Smith et al., 1996). In addition, the NOESY spectrum is consistent with an α-helical conformation in this zone (Figures 5A and 5C). The medium or strong NH(i)-NH(i+1) and medium H_α(i)-NH(i+3) NOE crosspeaks are typical of α helices. The decrease of the temperature stabilizes the helical

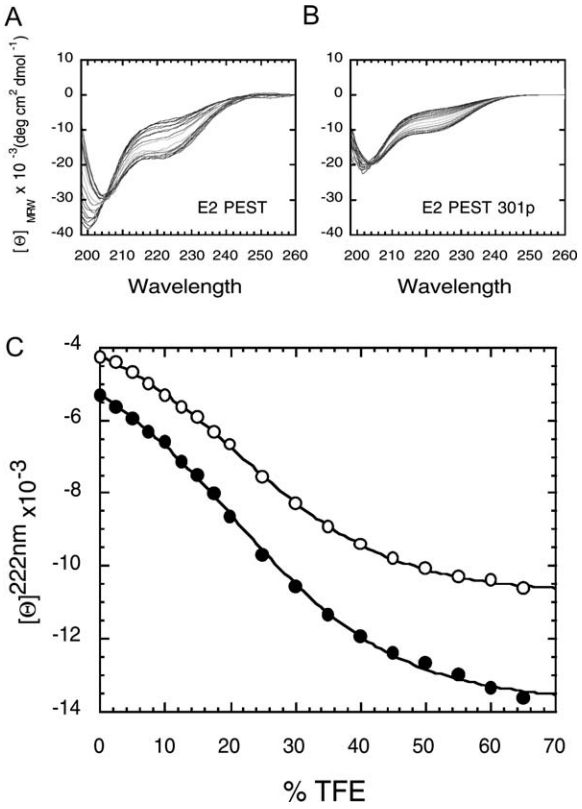

Figure 4. Stabilization of α-Helical Populations in BPV1 E2-PEST Peptides by TFE

(A and B) Far-UV circular dichroism of (A) E2-PEST and (B) E2-PEST301p at different TFE concentrations ranging from 0% to 65% v/v at pH 4.5.

(C) Molar ellipticity at 222 nm E2-PEST (black circle) and E2-PEST301p (white circle) as a function of the percentage of TFE (v/v).

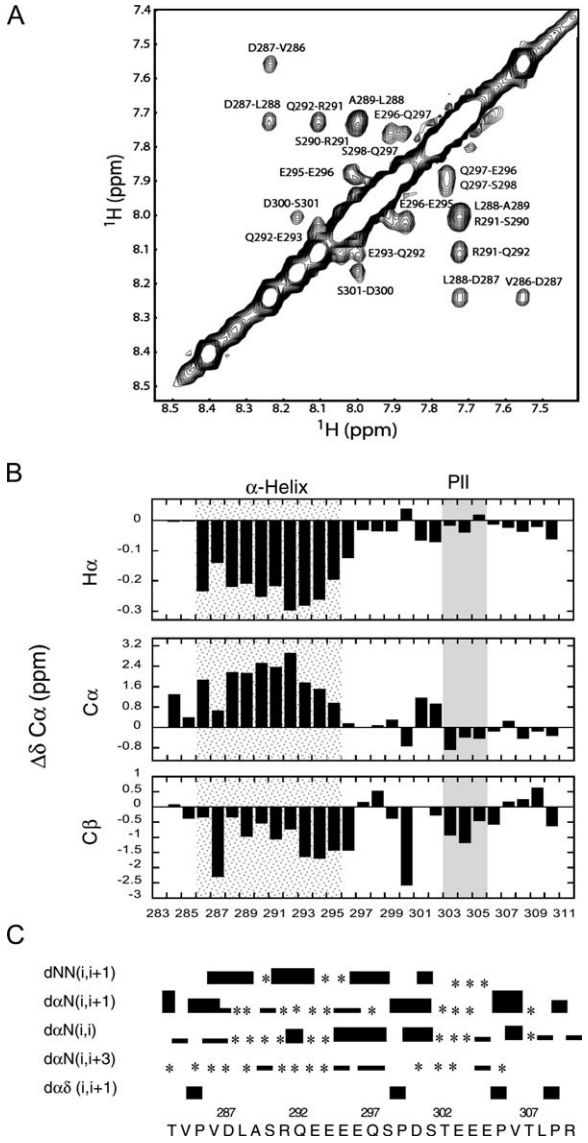

Figure 5. Structural Characterization of E2-PEST in Solution

(A) Backbone amide region of the ^{1}H-NOESY spectrum of the E2-PEST peptide at 25ºC (pH 4.5) in 1:1 TFE:H_2O. The sequential NH-NH connectivity is shown.

(B) Plot of the chemical shift differences between the observed resonances and values found in a random coil conformation, $\Delta\delta = \delta$ (observed) $- \delta$ (random coil), versus the position along the peptidic sequence for $^{1}H_{\alpha}$, $^{13}C_{\alpha}$, and $^{13}C_{\beta}$ on the top, medium, and lower panels, respectively. The tracts with defined elements of secondary structure are shaded on the plot.

(C) Summary of sequential and medium-range NOEs involving $N^{1}H$ and $^{1}H_{\alpha}$ protons. Strong, medium, and weak NOEs, classified according to the intensity of the crosspeak, are indicated by the different heights of the connecting boxes. The asterisks represent the NOEs that cannot be assigned due to the signal overlap. Bottom line: $H_{\alpha}(i)$-$H_{\delta}(i+1)$ NOEs for proline residues, indicating that all of the prolines are in a *trans* conformation, are also shown.

conformation; in particular, $^{1}J_{CH\alpha}$ coupling constants were increased at 10ºC with respect to 25ºC (Figure 7B). In water, the helix showed a dynamic behavior, where the chemical shifts of the corresponding α-helical residues resemble those of random coil and the characteristic NOE crosspeaks are relatively less intense (data not shown). In contrast to TFE, the Gdm.Cl completely disrupts the α helix. Both chemical shifts (data not shown) and $^{1}J_{CH\alpha}$ (Figure 7C; Table 2) approached random coil values.

The far-UV CD spectrum indicated that the peptide has regions of poly-proline-type (PII) structure. The PII is an extended left-handed helix that does not exhibit characteristic proton or carbon chemical shift deviations from random coil values as found in α helix and β sheet conformations (Shi et al., 2002a). Due to the absence of main chain hydrogen bonds in PII helices, detection of this type of structure is not possible from inter-residue amide-amide NOEs. A recent paper (Lam and Hsu, 2003) proposed a strategy based on nitrogen chemical shifts and, especially, scalar coupling constants to identify PII helices in the presence of other structure elements. The difference between measured $^{1}J_{CH\alpha}$ and random coil values characteristic of PII helices is reported to be larger than 1.1 Hz (Lam and Hsu, 2003). In contrast, the mean differences in $^{1}J_{CH\alpha}$ for α helix are 4.8 Hz (Vuister et al., 1992). For $^{3}J_{NHH\alpha}$, the difference between observed and random coil values for PII is smaller than −0.7 (Lam and Hsu, 2003), and the difference is smaller than −2.4 for α helix (Smith et al., 1996). Furthermore, PII helices show a unique denaturant-mediated stabilization, particularly strong at lower temperatures.

Table 2. Difference between the Observed Scalar Coupling Constants and the Random Coil Values for E2-PEST

	$\Delta^3J_{NHH\alpha}$[a]	$\Delta^1J_{C\alpha H\alpha}$[b]	
Residue	1:1 TFE:H_2O	1:1 TFE:H_2O	2 M Gdm.Cl[c]
V284	−0.7	0.8	0.7
P285		Nd	1.2
V286	−2.6	1.9	1.5
D287	−2.1	2.1	−0.5
L288	−3.1	4.1	2.1
A289	−2.1[d]	1.5	−0.9
S290	−1.7	3.7	1.1
R291	−2.7	4.3	−0.7
Q292	−2.0	4.0	0.1
E293	−2.8[d]	3.8	−0.3
E294	−2.3	2.7	0.5
E295	−1.7	1.8	−0.3
E296	−1.7	0.9	−0.2
Q297	−2.0	0.9	0.6
S298	−0.7	0.7	2.7
P299		Nd	−1.2
D300	−1.5	3.5	1.1
S301	−2.7[d]	1.7	0.7
T302	−2.5	1.1	1.3
E303	−1.1	1.7	2.9
E304	−1.1	1.2	3.7
E305	−1.1	1.1	2.5
P306		0.5	1.2
V307	−0.7	−0.3	−1.6
T308	−0.6	−0.4	−1.8
L309	−0.1	2.0	0.1
P310		−0.1	−2.4

Values are measured at 25ºC in a 1:1 TFE:H_2O and in 2 M Gdm.Cl as indicated. Nd: not determined.
[a] Random coil values were from Smith et al. (1996).
[b] Random coil values were from Vuister et al. (1992).
[c] The constant values of residues E293 and E294, E295 and E296, P306 and P310, and P285 and P299 in the guanidinium solution may be exchangeable.
[d] Minimal value.

The C-terminal region of the peptide (P299-R311) displayed chemical shift values consistent with the absence of α helix or β sheet structure. The signal overlap observed for the glutamic acid repeat excluded a complete analysis of the NOESY spectrum. Nevertheless, based on the difference between observed and random coil values for the $^3J_{NHH\alpha}$ and the $^1J_{CH\alpha}$ constants (Table 2), our data are indicative of a PII conformation in the region spanning the E303-E304-E305 residue tract of the peptide. In this region and at 25ºC in 1:1 water:TFE, $^3J_{NHH\alpha}$ values are smaller and $^1J_{CH\alpha}$ values are larger than random coil values (Table 2). The differences in $^1J_{CH\alpha}$ values measured were 1.7, 1.2, and 1.1 Hz for E303, E304, and E305, respectively. Differences in $^3J_{NHH\alpha}$ at the same temperature were −1.1 Hz for the 3 residues mentioned. T302 may possibly be in a PII conformation; though the $^3J_{NHH\alpha}$ value is quite small ($^1J_{CH\alpha}$ is 1.1 Hz, and $^3J_{NHH\alpha}$ is −2.5 Hz). Also, the narrow NH chemical shift range observed (7.94–7.98 ppm) is consistent with solvent-exposed amide protons not involved in hydrogen bonding, and it further supports the presence of the PII structure in this region. In addition, $^1J_{CH\alpha}$ values were observed to increase with the decrease in temperature (Figure 7B), as observed for other PII-containing peptides (Shi et al., 2002b). A distinctive behavior of PII helices is that they can be stabilized by denaturants (Shi et al., 2002a). In fact, the E303-E305 tract of PEST showed an increase of $^1J_{CH\alpha}$ values in 2.0 M Gdm.Cl, whereas all other residues, including those of the α helix, showed values very close to those of random coil (Figure 7C).

A salient feature in E2-PEST is the small value of the $^3J_{NHH\alpha}$ coupling constant for S301 and the large value for the $^1J_{CH\alpha}$ coupling constant for D300, strongly suggesting the presence of a turn-type structure around this amino acid. The presence of this turn is consistent with the observed medium NH(D300)-NH(S301) NOE crosspeak (Figures 5A and 5C), and this will have structural and thermodynamic implications when this serine is phosphorylated (see below). Summarizing, the NMR data indicated that the E2-PEST peptide presents two characteristic secondary structure elements: an α helix in V286-E296 and a PII helix in E303-E305. The presence of a turn around P299 would mediate an interaction between both tracts.

Phosphorylation of the E2-PEST Peptide Destabilizes both PII and the α Helix

To further define the structural link between phosphorylation and thermodynamic stability in the PEST region of BPV1 E2 as the basis for the increased turnover in the cell (Penrose et al., 2004), we tackled an NMR study of the E2-PEST301p. Far-UV CD spectra showed a destructuration of the peptide upon phosphorylation of S301, with a decrease in α-helical content (Figure 4; Table 1). A series of 2D NMR spectra on E2-PEST301p were carried out in similar conditions to the unphosphorylated peptide, and the chemical shifts were assigned (Figure 6A; Table S1; see the Supplemental Data available with this article online). Figure 6B shows the difference between C_α chemical shift values observed for E2-PEST and E2-PEST301p peptides (at 25ºC). A major difference is, not surprisingly, found around the phosphorylation site, S301. The regions of the α helix and PII also present significant variation in the chemical shift values indicative of local structure perturbation. The difference with random coil values decreased for the entire length of the α helix and for the PII tract. These results confirm a destabilization of the structure of the peptide, including the α and the PII helices, caused by the phosphorylation of S301.

The $^1J_{C\alpha H\alpha}$ and $^3J_{NHH\alpha}$ coupling constants were also determined for the phosphorylated E2-PEST301p peptide (Table 2; Table S1). The results were consistent with the chemical shift analysis, indicating a destructuration of E2-PEST upon phosphorylation, as differences with random coil values are smaller for the phosphorylated peptide for α helix and PII tracts. We use the $^1J_{C\alpha H\alpha}$ values of E2-PEST in the TFE:H_2O solution at 25ºC as a reference to analyze the effect of the phosphorylation of S301, and we compared it with the observed effect of temperature and Gdm.Cl on the structured regions (Figure 7). A negative value for the $^1J_{C\alpha H\alpha}$ difference indicates destabilization of either the α helix or PII conformations with respect to the E2-PEST peptide in the reference conditions. In the case of phosphorylation, the difference between the constant values is negative for both regions (Figure 7A), indicating a destabilization of both α helix and PII regions. The loss of structure is located mainly in the C-terminal half of the α helix, from

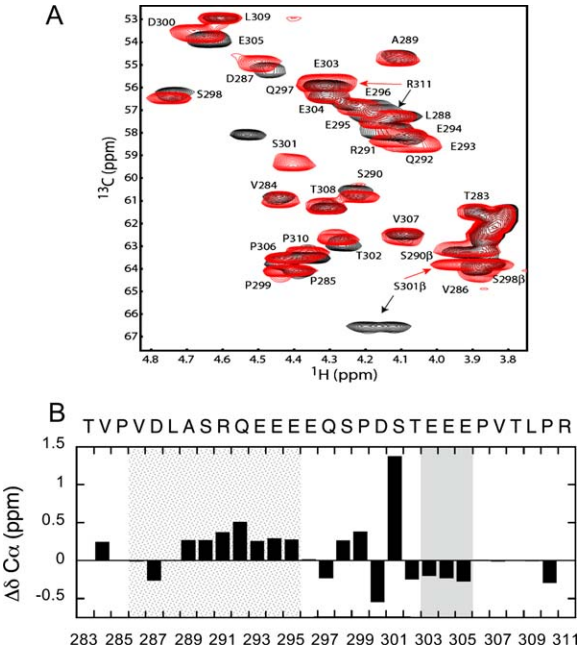

Figure 6. Effect of Phosphorylation on the Structure of the E2-PEST Peptide

(A) Overlapping of the $^{13}C_{\alpha}$-$^{1}H_{\alpha}$ region of the [^{13}C,^{1}H]-HSQC spectra at natural abundance of E2-PEST (red) and E2-PEST301p (black) peptides.

(B) Plot of the differences between $^{13}C_{\alpha}$ chemical shifts observed between E2-PEST and E2-PEST301p peptides at 25ºC, $\Delta\delta C_{\alpha}$ = δC_{α}(E2-PEST) − δC_{α}(E2-PEST301p), plotted against the position along the full-length E2 sequence. The value for S301 is out of scale. The tracts with defined elements of secondary structure are shaded on the plot.

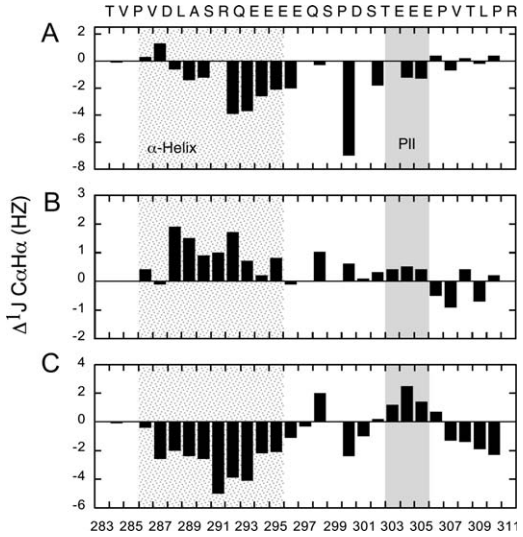

Figure 7. Effect of Temperature, Gdm.Cl, and Phosphorylation on E2-PEST

(A–C) Plot of the differences between the $^{1}J_{C\alpha H\alpha}$ values for: (A) E2-PEST and E2-PEST301p, $\Delta^{1}J_{C\alpha H\alpha}$ = $^{1}J_{C\alpha H\alpha}$ (E2-PEST301p) − $^{1}J_{C\alpha H\alpha}$ (E2-PEST), at 25ºC in a 1:1 TFE:H_2O solution at pH 4.5; (B) E2-PEST at 25ºC and at 10ºC, $\Delta^{1}J_{C\alpha H\alpha}$ = $^{1}J_{C\alpha H\alpha}$ (E2-PEST at 10ºC) − $^{1}J_{C\alpha H\alpha}$ (E2-PEST at 25ºC), in a 1:1 TFE:H_2O solution at pH 4.5; and (C) E2-PEST in 2 M Gdm.Cl and in a 1:1 TFE:H_2O solution, Δ $^{1}J_{C\alpha H\alpha}$ = $^{1}J_{C\alpha H\alpha}$ (E2-PEST in Gdm.Cl) − $^{1}J_{C\alpha H\alpha}$ (E2-PEST in TFE:H_2O), at 25ºC and pH 4.5. (The constant values of residues E293 and E294, E295 and E296, P306 and P310, and P285 and P289 in the guanidinium solution may be exchangeable.) The tracts with defined elements of secondary structure are shaded on each plot and are depicted above the sequence.

Q292 to E296. A large difference in $^{1}J_{C\alpha H\alpha}$ is observed for residue D300, the residue adjacent to the phosphorylation site, whose $^{1}J_{C\alpha H\alpha}$ in the TFE:H_2O solution is anomalously large for the unphosphorylated peptide. This unequivocally corresponds to a conformational change upon phosphorylation, most likely related to the presence of a turn around residue P299, as was suggested by the CD analysis of the P299A peptide. The effect of phosphorylation and/or mutation on the secondary structure of the E2-PEST is even clearer when the difference in $^{1}J_{C\alpha H\alpha}$ is compared with the effect of temperature and Gdm.Cl; the decrease in temperature shows increased values for the difference in $^{1}J_{C\alpha H\alpha}$, indicative of stabilization of both α-helical and PII regions (Figure 7B). In contrast, Gdm.Cl causes a decrease on the $^{1}J_{C\alpha H\alpha}$ in the entire α helix, indicative of the expected unfolding effect of the denaturant on this type of structure; however, the PII region is stabilized by Gdm.Cl, with the consequent increment of the difference in $^{1}J_{C\alpha H\alpha}$ (Figure 7C).

Discussion

Given the widespread distribution of PEST sequences in proteins from all kingdoms (Rechsteiner and Rogers, 1996), establishing a model structure by which to study the effect of phosphorylation on protein conformation is most relevant. Protein degradation regulates processes such as gene transcription, cell cycle progression, circadian rhythms, inflammation, carcinogenesis, cholesterol metabolism, and antigen processing (Kornitzer and Ciechanover, 2000; Hampton, 2002; Yewdell and Princiotta, 2004). The PEST sequence within the nonconserved "hinge" domain of the bovine papillomavirus E2 protein is an ideal model, particularly because of the information available that correlates peptide structure and post-translational modification with protein stability and degradation within the cell (Penrose et al., 2004), which, in turn, regulates an essential feature in the viral life cycle such as episomal viral DNA copy number. Thus, we can link the effect of phosphorylation of a PEST sequence on peptide structure with its intracellular half-life.

The region linking C-terminal DNA recognition and N-terminal transactivation domains of BPV1 E2 was defined as flexible based on the absence of sequence conservation, a conclusion supported by the difficulty in crystallizing it for structure determination by X-ray crystallography (Gauthier et al., 1991). In this work, we describe that a peptide fragment comprising the PEST region in the hinge domain of BPV1 E2 protein contains elements of persistent structure that are disrupted by phosphorylation. This was investigated by both circular dichroism and NMR, which allowed characterization in solution and stabilization of the preexisting structures by modifications in the solvent composition. The unphosphorylated E2-PEST peptide is not disordered; it contains a dynamic α helix in water that is, on average, 3–4 residues long, and NMR indicates that it corresponds to the N-cap of the helix and is possibly stabilized by interaction with the preceding residues. Far-UV spectral characteristics and the response to pH,

temperature, and Gdm.Cl indicate the presence of a PII-type structure, in which E2-PEST appears as a natural poly-E model. While the PII population is increased at pH above 7.0, the opposite is true for α helix. The α-helical structure is stabilized in TFE, and NMR results show that it spans 11 residues, V286–E296. This is identical to the number of residues estimated from the TFE titration results, thus validating the solvent stabilization approach (Table 1). Similarly, residues E303–E305, and possibly also T302, appear in PII conformation. The α-helical and PII regions of the structure are interrupted by a turn-type structure centered around the proline residue at position 299 (P299).

Native proteins need to be unfolded for degradation, and their global or local stabilization prevents their proteolysis (Lee et al., 2001; Johnston et al., 1995). The structural features of the degradation initiation sites are not those found in a compact globular domain, but they are exposed and provide the necessary marginal stability that allows a fast and efficient destabilization, in this case acquired by phosphorylation. In addition, PII structures are emerging as major participants in unfolded states or in exposed regions of proteins (Shi et al., 2002b), and they play a key role in defining extended and accessible conformations for chemical modification and proteolysis (Iakoucheva et al., 2004). Phosphorylation of either or both S301 and S298 affects the structural stability of the E2-PEST peptide, although the dominant residue appears to be S301. The TFE titrations show that the α helix is destabilized in the double-phosphorylated peptide to a larger extent than the individually modified peptides (Table 1). This is understandable because S298 lies at the C-terminal cap of the α helix and S301 is located in the turn that links the α-helical and PII structures. On the other hand, only phosphorylation of S301 affects the PII content (Table 1), and this destabilization correlates most with the in vivo degradation results (Penrose et al., 2004).

NMR spectroscopy is the most powerful technique by which to define the dynamic structures present in flexible peptide fragments such as the E2-PEST peptide, which is in solution but isolated from a compact, folded protein. In the absence of a cooperative and compact structure, chemical shifts, NOE pattern analysis, and, as shown to be the most sensitive, analysis of coupling constants can be used to investigate this region in detail. The $^{1}J_{C\alpha H\alpha}$ and $^{3}J_{HN\alpha}$ constants of E2-PEST301p approach random coil values for the region of the PII (E303-E304-E305), and they indicate an important loss of PII conformation upon phosphorylation (Figure 7; Table 2). Most of the helix, in particular that present near the C-cap, is also affected by phosphorylation. A decrease of α helix propensity as a consequence of phosphorylation has previously been reported (Andrew et al., 2002), especially when the phosphorylated residue is next to the C terminus of the helix. The NOE spectra support this assumption, because the sequential NH(i)-NH(i+1) crosspeaks in the α helix are relatively less intense in the case of the phosphorylated amino acid. Taken together, these results point to destabilization of the structure of the phosphorylated peptide. A turn around P299 would allow an interaction between the α helix and the PII-type structure involving S301, and the phosphorylation of this residue would affect this interaction and therefore the overall conformation of the peptide. Significantly low and high values of $^{3}J_{HN\alpha}$ and $^{1}J_{C\alpha H\alpha}$, respectively, were observed in the unphosphorylated form, and the medium NOE NH(i)-NH(i+1) between residues D300 and S301 suggests the presence of the turn that is stabilized at a lower temperature. Figure 8 summarizes the results presented here on the effect of phosphorylation on the structure of the E2-PEST peptide in solution.

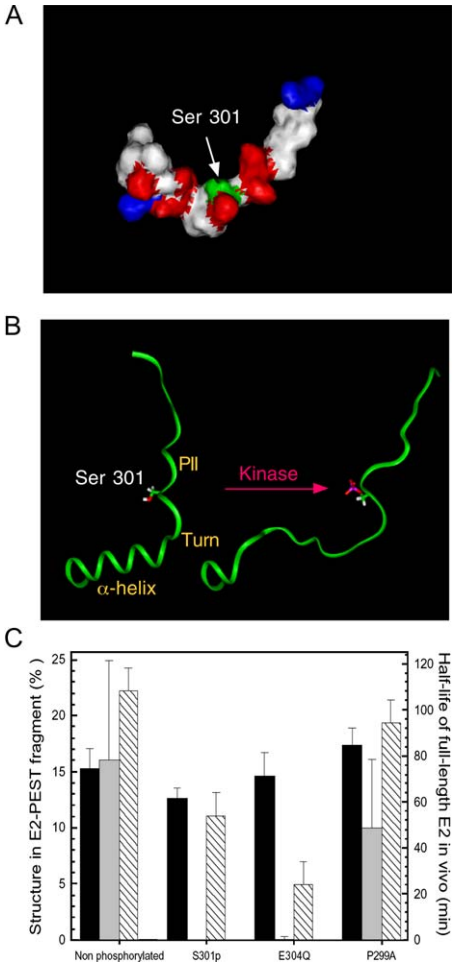

Figure 8. Phosphorylation Triggers the Conformational Switch Required for Degradation

(A) Electrostatic potential surface representation of E2-PEST. Red, negative; blue, positive; white, neutral; green, serine 301.

(B) Model based on the structural features of the E2-PEST, showing the α helix, turn, and PII structures (left) that are disrupted after phosphorylation of S301 (right, S301 is depicted in backbone, and the phosphate added is marked in pink).

(C) Correlation between the half-lives of full-E2 proteins in vivo and the structure content in E2-PEST fragments. Data of percent α helix content (black) in water was obtained from Table 1. PII content (gray) was calculated from ΔG values of PII formation from Table 1 (see Experimental Procedures). Half-lives of full-length E2 proteins in vivo from Table 1 are shown (diagonal stripes). The half-life of unphosphorylated E2 cannot be calculated experimentally since it is not possible to discriminate between the phosphorylated and unphosphorylated species. The best estimate for this is the S290,S298,S301AAA triple mutant, since it cannot be phosphorylated by CKII (Penrose et al., 2004). Phosphorylation on S301 of the wild-type and S298A full-length E2 proteins is responsible for the accelerated turnover (Penrose et al., 2004), and therefore the half-life values for these species can be associated to the E2-PEST301p fragment.

Two mutations were selected for the analysis of the correlation between thermodynamic stability and stability leading to degradation in the cell (Penrose et al., 2004). The E2 protein containing the E304Q substitution showed a fast turnover even in the absence of phosphorylation, and in the corresponding E2-PEST peptide the PII conformation was largely disrupted, in water or in 50% TFE (Figure 3; Table 1), without altering the α helix. On the other hand, the P299A E2 protein showed a largely increased half-life that was virtually unaffected by phosphorylation (slow turnover) (Penrose et al., 2004). The corresponding peptide had increased α-helical content, which was not unexpected due to the replacement of the proline residue, which favors the turn. The α-helical content showed a slight increase of 14% in water, in agreement with algorithm predictions (Munoz and Serrano, 1995) (data not shown), but a very large increase (74%) in TFE, resulting from the recruitment of 8 additional residues into the α-helical conformation. Thus, this suggests that in water, the helix is extended for a few residues into the previously existing turn, but it does not disrupt the neighboring PII structure. In 50% TFE, however, the entire region adopts an "artificial" α helix conformation that is 19 residues long. In the context of the full protein, this mutation protects E2 from degradation by stabilizing the structure of the entire PEST region. Furthermore, this structure is now impervious to disruption by phosphorylation.

Regulation of proteolytic degradation by a disruption of local protein structure is a fast and effective way to control the activities of this transcriptional regulator with important consequences for the viral life cycle. In the same way that CK1 and CK2 are not very selective in terms of substrate specificity, the resulting destabilized structures need not adopt a particular conformation to be recognized by proteasome elements or other proteases. Such local unfolding could render the polypeptide susceptible to cleavage by proteases in general; after all, the proteolytic activities in the proteasome are not highly specific. In fact, PEST motifs can also be targets of calpain (Martinez et al., 2003; Shumway et al., 1999). A local destabilization product of phosphorylation at a PEST site may increase the accessibility of lysine residues to ubiquitination, with the consequent increase in proteasome degradation of the targeted protein. However, recent work showed that an unstructured initiation site is required for efficient proteasome degradation in addition to ubiquitin modification, which serves mainly as a recognition event (Prakash et al., 2004). In addition to chaperone unfoldase activity, another way to generate such local destabilization in the protein could be a phosphorylation event such as the one described here, in which the PEST motif acts as an initiation site. Moreover, initiation sites next to an α helix or flexible structures such as those we describe here are more easily unfolded and degraded when compared to initiation sites next to the β strand structure (Lee et al., 2001). In this respect, phosphorylation is often related exclusively to the generation of a "label" to be recognized by a target protein or receptor. The present work suggests that, in the case of the dynamic PEST regions, what the phosphate modification does is to disrupt the local thermodynamic conformational equilibrium. Therefore, the fate of the PEST-carrying protein will be dictated by the stability of that region, whether it is strictly local or participates in long-range interactions with other domains, and not by the phosphate recognition by a target. Further analysis of other PEST sequences will be required to confirm this.

The correlation found between structural stability and this posttranslational modification results is essential for protein function determination. Although in most cases the basal state of a PEST motif is unphosphorylated, in some cases the major species are phosphorylated (Rechsteiner and Rogers, 1996). This suggests that conformational equilibria of the kind described here could also be modulated by phosphatases. Studies extending the effect of modifications other than phosphorylation will provide insight into the evolution of the widely distributed PEST regions or other extended sequences containing PII structure and insight into how these are modulated by a chemical modification acting as a conformational trigger.

Experimental Procedures

Chemicals

E2-PEST peptides were synthesized, purified, and quantified as previously described (Penrose et al., 2004). 2,2,2 Trifluoroethanol and Gdm.Cl were purchased from ICN, Biomedicals, Inc. All other reagents were of the highest purity available.

Circular Dichroism

Spectra were obtained by using a Jasco J-815 instrument with cell paths of 0.1 and 0.5 mm. Peptide concentration was 20 μM under conditions described. Five far-UV scans were averaged, and the buffer baseline was subtracted from all spectra registered. Temperature was kept within ±0.1ºC by using a peltier device, and curves, with a slope of 5ºC/min and ranging from 2ºC to 90ºC, were carried out in 10 mM Tris-HCl buffer (pH 7.5); spectra were taken every 5ºC. For TFE and Gdm.Cl titrations, 10 mM Tris-HCl (pH 7.5) or Sodium Formiate (pH 4.5) were used as indicated, while 10 mM Citrate-phosphate buffer (pH 3.0, 4.0, 5.0, 6.0, 7.0, and 8.0) was used in the pH titration curve.

Estimation of PII and α-Helical Content

The conformational equilibria involving PII, coil, and α helix for a peptide in water can be determined by using Equation 1 (Park et al., 1997):

$$[\Theta] = f\,\mathrm{H}\,[\Theta]\mathrm{H} + f\,\mathrm{PII}\,[\Theta]\mathrm{PII} + f\,\mathrm{U}\,[\Theta]\mathrm{U}, \quad (1)$$

where *f* H, *f* PII, and *f* U are the α-helical, PII, and unstructured conformations, respectively, and [Θ]H, [Θ]PII, and [Θ]U are the mean residue ellipticities of these conformations; there are no definitive values for [Θ]PII and [Θ]U. Alternatively, Equation 1 can be represented with different equilibria, by assuming a two-state transition between the α helix or PII to coil state and by using solvent conditions that are known to stabilize either the α helix (Nelson and Kallenbach, 1986) or the PII (Tiffany and Krimm, 1968) conformations. Equation 2 (Pace, 1986) is used to estimate the thermodynamic parameters of each structure:

$$\Delta G_x = \Delta G_{H2O} - m[x], \quad (2)$$

where ΔG_x is the free energy of α helix or PII formation of the peptide in TFE/H_2O or [Gdm.Cl], ΔG_{H2O} is the free energy in water, and [*x*] is the molar ratio of [TFE]/[H_2O] or [Gdm.Cl] as indicated. The molar ellipticity of each peptide as a function of the concentration of TFE or Gdm.Cl is fitted to the equation proposed for the TFE binding model (Jasanoff and Fersht, 1994), where the mean residue ellipticity at 222 nm $[\Theta]_{222}$ in this case is used for determining either the α helix or PII populations. The fitting was performed by using Kaleidagraph software (Ablebeck).

TFE and Gdm.Cl Titrations

For TFE experiments, the peptides were dissolved in 0%–65% TFE (v/v) and 20 mM Sodium Formiate (pH 4.5). The α helix percentage in TFE is estimated according to a standard empirical equation (de Prat-Gay, 1997). For Gdm.Cl titrations, spectra were recorded at 20ºC with different concentrations of the denaturant (from 0 to 6.5 M Gdm.Cl) in 10 mM Tris-HCl (pH 7.5). $\Delta\Theta$ is the difference between the molar ellipticity of the peptide for a given Gdm.Cl concentration and 0 M Gdm.Cl at 222 nm.

NMR

E2-PEST and E2-PEST301p peptides (2.5 mM) were dissolved in a 50% TFE-*d*3, 50% 20 mM sodium acetate (pH 4.5) solution, and E2-PEST was also dissolved in 20 mM sodium acetate (pH 4.5) solution (10% D_2O was added) and in 2 M Gdm.Cl solution (pH 4.5), 10% D_2O. The NMR experiments were performed at 10ºC or 25ºC with Bruker Avance 700 and Avance 400 spectrometers equipped with triple-resonance probes incorporating self-shielded gradient coils. All of the heteronuclear correlation experiments were carried out at natural abundance. Pulsed-field gradients were appropriately employed to achieve suppression of the solvent signal and spectral artifacts. Quadrature detection in the indirectly detected dimensions was obtained by using the States-TPPI method (Marion and Wuthrich, 1983) or the echo-antiecho method, and the spectra were processed on Silicon Graphics workstations by the NMRPipe software (Delaglio et al., 1995) and were analyzed with NMRView (Johnson and Blevins, 1994). All of the proton and carbon resonances were assigned by 2D spectra: TOCSY (mixing time 60 ms) to identify the spin systems (Bax and Davis, 1985), [^{1}H-^{13}C] HMQC (Bax et al., 1983) and [^{1}H-^{13}C] HMQC-TOCSY (with a mixing time of 40, 60, and 80 ms) to assist with crosspeaks assignment (Braunschweiler and Ernst, 1983), and NOESY (with a mixing time of 0.150 s and 0.250 s) (Bax and Davis, 1985), according to the sequential assignment method (Wuthrich, 1986). ^{15}N chemical shifts were measured from a natural abundance [^{15}N-^{1}H] HSQC experiment (Grzesiek and Bax, 1993). The $^1J_{C\alpha H\alpha}$ coupling constants values were measured from the in-phase splitting patterns of the C_α-H_α crosspeaks in the HMQC spectra without carbon decoupling. The $^3J_{HNH\alpha}$ values were measured from the in-phase splitting patterns of the NH-C crosspeaks in the [^{1}H-^{13}C] HSQC-TOCSY spectrum collected with 8k complex data points in F2.

Supplemental Data

Supplemental Data including NMR data, scalar coupling constant values, chemical shifts, and assignments for E2-PEST peptides are available at http://www.structure.org/cgi/content/full/14/2/309/DC1/.

Acknowledgments

M.M.G.-A. holds a Ph.D. studentship from the University of Buenos Aires, and D.E.W. holds a post-doctoral fellowship from CONCIET. G.P.G. is a career investigator from CONCIET. This work was supported in part by Wellcome Trust CRIG OIA U41 RG27994 and ANPCyT grant PICT 2002 0110944. We thank Jonathan Spindler for data analysis of E2 half-lives.

Received: August 18, 2005
Revised: October 26, 2005
Accepted: November 4, 2005
Published: February 10, 2006

References

Andrew, C.D., Warwicker, J., Jones, G.R., and Doig, A.J. (2002). Effect of phosphorylation on α-helix stability as a function of position. Biochemistry *41*, 1897–1905.

Bax, A., and Davis, D.G. (1985). MLEV-17 based two-dimensional homonuclear magnetization transfer spectroscopy. J. Magn. Reson. *65*, 355–360.

Bax, A., Griffey, R.H., and Hawkins, B.L. (1983). Correlation of proton and nitrogen-15 chemical shifts by multiple quantum NMR. J. Magn. Reson. *55*, 301–315.

Belvin, M.P., Jin, Y., and Anderson, K.V. (1995). Cactus protein degradation mediates *Drosophila* dorsal-ventral signaling. Genes Dev. *9*, 783–793.

Braunschweiler, L., and Ernst, R.R. (1983). Coherence transfer by isotropic mixing: application to proton correlation spectroscopy. J. Magn. Reson. *55*, 521–528.

Buck, M. (1998). Trifluoroethanol and colleagues: cosolvents come of age. Recent studies with peptides and proteins. Q. Rev. Biophys. *31*, 297–355.

Chen, Y.H., Yang, J.T., and Chau, K.H. (1974). Determination of the helix and beta form of proteins in aqueous solution by circular dichroism. Biochemistry *13*, 3350–3359.

Delaglio, F., Grzesiek, S., Vuister, G.W., Zhu, G., Pfeifer, J., and Bax, A. (1995). NMRPipe: a multidimensional spectral processing system based on UNIX pipes. J. Biomol. NMR *6*, 277–293.

de Prat-Gay, G. (1997). Conformational preferences of a peptide corresponding to the major antigenic determinant of foot-and-mouth disease virus: implications for peptide-vaccine approaches. Arch. Biochem. Biophys. *341*, 360–369.

Gauthier, J.M., Dillner, J., and Yaniv, M. (1991). Structural analysis of the human papillomavirus type 16–E2 transactivator with antipeptide antibodies reveals a high mobility region linking the transactivation and the DNA-binding domains. Nucleic Acids Res. *19*, 7073–7079.

Grzesiek, S., and Bax, A. (1993). The importance of not saturating water in protein NMR: application to sensitivity enhancement and NOE measurements. J. Am. Chem. Soc. *115*, 12593–12594.

Hampton, R.Y. (2002). Proteolysis and sterol regulation. Annu. Rev. Cell Dev. Biol. *18*, 345–378.

Howley, P. (2001). Papillomaviruses and their replication. In Fields Virology, Fourth Edition, D.M. Knipe and P.M. Howley, eds. (Philadelphia: Lippincot Williams and Wilkins), pp. 2197–2229.

Iakoucheva, L.M., Radivojac, P., Brown, C.J., O'Connor, T.R., Sikes, J.G., Obradovic, Z., and Dunker, A.K. (2004). The importance of intrinsic disorder for protein phosphorylation. Nucleic Acids Res. *32*, 1037–1049.

Jasanoff, A., and Fersht, A.R. (1994). Quantitative determination of helical propensities from trifluoroethanol titration curves. Biochemistry *33*, 2129–2135.

Johnson, B.A., and Blevins, R.A. (1994). A computer program for the visualization and analyses of NMR data. J. Biomol. NMR *4*, 603–614.

Johnston, J.A., Johnson, E.S., Waller, P.R., and Varshavsky, A. (1995). Methotrexate inhibits proteolysis of dihydrofolate reductase by the N-end rule pathway. J. Biol. Chem. *270*, 8172–8178.

Kornitzer, D., and Ciechanover, A. (2000). Modes of regulation of ubiquitin-mediated protein degradation. J. Cell. Physiol. *182*, 1–11.

Lam, S.L., and Hsu, V.L. (2003). NMR identification of left-handed polyproline type II helices. Biopolymers *69*, 270–281.

Lee, C., Schwartz, M.P., Prakash, S., Iwakura, M., and Matouschek, A. (2001). ATP-dependent proteases degrade their substrates by processively unraveling them from the degradation signal. Mol. Cell *7*, 627–637.

Liu, Z., Chen, K., Ng, A., Shi, Z., Woody, R.W., and Kallenbach, N.R. (2004). Solvent dependence of PII conformation in model alanine peptides. J. Am. Chem. Soc. *126*, 15141–15150.

Marion, D., and Wuthrich, K. (1983). Application of phase sensitive two-dimensional correlated spectroscopy (COSY) for measurements of 1H–1H spin-spin coupling constants in proteins. Biochem. Biophys. Res. Commun. *113*, 967–974.

Martinez, L.O., Agerholm-Larsen, B., Wang, N., Chen, W., and Tall, A.R. (2003). Phosphorylation of a pest sequence in ABCA1 promotes calpain degradation and is reversed by ApoA-I. J. Biol. Chem. *278*, 37368–37374.

McBride, A.A., and Howley, P.M. (1991). Bovine papillomavirus with a mutation in the E2 serine 301 phosphorylation site replicates at a high copy number. J. Virol. *65*, 6528–6534.

Munoz, V., and Serrano, L. (1995). Elucidating the folding problem of helical peptides using empirical parameters. III. Temperature and pH dependence. J. Mol. Biol. *245*, 297–308.

Myers, J.K., Pace, C.N., and Scholtz, J.M. (1995). Denaturant m values and heat capacity changes: relation to changes in accessible surface areas of protein unfolding. Protein Sci. *4*, 2138–2148.

Nelson, J.W., and Kallenbach, N.R. (1986). Stabilization of the ribonuclease S-peptide α-helix by trifluoroethanol. Proteins *1*, 211–217.

Pace, C.N. (1986). Determination and analysis of urea and guanidine hydrochloride denaturation curves. Methods Enzymol. *131*, 266–280.

Park, S.H., Shalongo, W., and Stellwagen, E. (1997). The role of PII conformations in the calculation of peptide fractional helix content. Protein Sci. *6*, 1694–1700.

Penrose, K.J., and McBride, A.A. (2000). Proteasome-mediated degradation of the papillomavirus E2-TA protein is regulated by phosphorylation and can modulate viral genome copy number. J. Virol. *74*, 6031–6038.

Penrose, K.J., Garcia-Alai, M., de Prat-Gay, G., and McBride, A.A. (2004). Casein Kinase II phosphorylation-induced conformational switch triggers degradation of the papillomavirus E2 protein. J. Biol. Chem. *279*, 22430–22439.

Prakash, S., Tian, L., Ratliff, K.S., Lehotzky, R.E., and Matouschek, A. (2004). An unstructured initiation site is required for efficient proteasome-mediated degradation. Nat. Struct. Mol. Biol. *11*, 830–837.

Rechsteiner, M. (1990). PEST sequences are signals for rapid intracellular proteolysis. Semin. Cell Biol. *1*, 433–440.

Rechsteiner, M. (1991). Natural substrates of the ubiquitin proteolytic pathway. Cell *66*, 615–618.

Rechsteiner, M., and Rogers, S.W. (1996). PEST sequences and regulation by proteolysis. Trends Biochem. Sci. *21*, 267–271.

Rogers, S., Wells, R., and Rechsteiner, M. (1986). Amino acid sequences common to rapidly degraded proteins: the PEST hypothesis. Science *234*, 364–368.

Sancho, J., Neira, J.L., and Fersht, A.R. (1992). An N-terminal fragment of barnase has residual helical structure similar to that in a refolding intermediate. J. Mol. Biol. *224*, 749–758.

Shi, Z., Olson, C.A., Rose, G.D., Baldwin, R.L., and Kallenbach, N.R. (2002a). Polyproline II structure in a sequence of seven alanine residues. Proc. Natl. Acad. Sci. USA *99*, 9190–9195.

Shi, Z., Woody, R.W., and Kallenbach, N.R. (2002b). Is polyproline II a major backbone conformation in unfolded proteins? Adv. Protein Chem. *62*, 163–240.

Shumway, S.D., Maki, M., and Miyamoto, S. (1999). The PEST domain of IκBα is necessary and sufficient for in vitro degradation by mu-calpain. J. Biol. Chem. *274*, 30874–30881.

Skiadopoulos, M.H., and McBride, A.A. (1998). Bovine papillomavirus type 1 genomes and the E2 transactivator protein are closely associated with mitotic chromatin. J. Virol. *72*, 2079–2088.

Smith, L.J., Bolin, K.A., Schwalbe, H., MacArthur, M.W., Thornton, J.M., and Dobson, C.M. (1996). Analysis of main chain torsion angles in proteins: prediction of NMR coupling constants for native and random coil conformations. J. Mol. Biol. *255*, 494–506.

Tiffany, M.L., and Krimm, S. (1968). New chain conformations of poly (glutamic acid) and polylysine. Biopolymers *6*, 1379–1382.

Tiffany, M.L., and Krimm, S. (1972). Effect of temperature on the circular dichroism spectra of polypeptides in the extended state. Biopolymers *11*, 2309–2316.

Tiffany, M.L., and Krimm, S. (1973). Extended conformations of polypeptides and proteins in urea and guanidine hydrochloride. Biopolymers *12*, 575–587.

Vuister, G.W., Delaglio, F., and Bax, A. (1992). An empirical correlation between ^{1}JCαHα and protein backbone conformation. J. Am. Chem. Soc. *114*, 9674–9675.

Wishart, D.S., and Sykes, B.D. (1994). Chemical shifts as a tool for structure determination. Methods Enzymol. *239*, 363–392.

Wuthrich, K. (1986). NMR of Proteins and Nucleic Acids (New York: Wiley-Interscience Publication).

Yewdell, J.W., and Princiotta, M.F. (2004). Proteasomes get by with lots of help from their friends. Immunity *20*, 362–363.